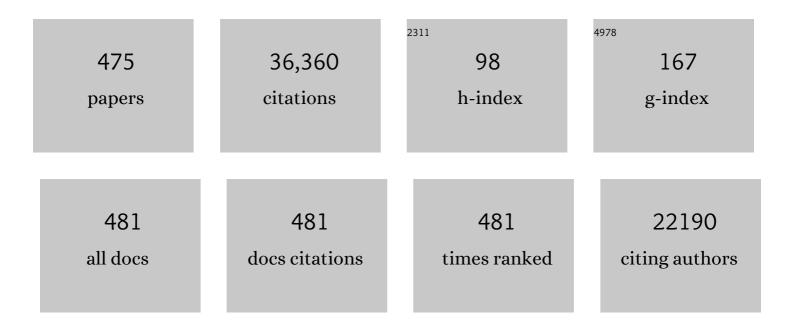
Shengzhong Frank Liu

List of Publications by Year in descending order

Source: https://exaly.com/author-pdf/5429361/publications.pdf Version: 2024-02-01



#	Article	IF	CITATIONS
1	High efficiency planar-type perovskite solar cells with negligible hysteresis using EDTA-complexed SnO2. Nature Communications, 2018, 9, 3239.	5.8	1,017
2	Twoâ€Inchâ€Sized Perovskite CH ₃ NH ₃ PbX ₃ (X = Cl, Br, I) Crystals: Growth and Characterization. Advanced Materials, 2015, 27, 5176-5183.	11.1	914
3	Surface optimization to eliminate hysteresis for record efficiency planar perovskite solar cells. Energy and Environmental Science, 2016, 9, 3071-3078.	15.6	870
4	Consensus statement for stability assessment and reporting for perovskite photovoltaics based on ISOS procedures. Nature Energy, 2020, 5, 35-49.	19.8	797
5	Stable Highâ€Performance Perovskite Solar Cells via Grain Boundary Passivation. Advanced Materials, 2018, 30, e1706576.	11.1	665
6	Stable high efficiency two-dimensional perovskite solar cells via cesium doping. Energy and Environmental Science, 2017, 10, 2095-2102.	15.6	588
7	High efficiency flexible perovskite solar cells using superior low temperature TiO ₂ . Energy and Environmental Science, 2015, 8, 3208-3214.	15.6	519
8	Allâ€Inorganic CsPbX ₃ Perovskite Solar Cells: Progress and Prospects. Angewandte Chemie - International Edition, 2019, 58, 15596-15618.	7.2	425
9	Hysteresisâ€5uppressed Highâ€Efficiency Flexible Perovskite Solar Cells Using Solidâ€5tate Ionicâ€Liquids for Effective Electron Transport. Advanced Materials, 2016, 28, 5206-5213.	11.1	387
10	All-inorganic cesium lead iodide perovskite solar cells with stabilized efficiency beyond 15%. Nature Communications, 2018, 9, 4544.	5.8	379
11	Record Efficiency Stable Flexible Perovskite Solar Cell Using Effective Additive Assistant Strategy. Advanced Materials, 2018, 30, e1801418.	11.1	377
12	Single atom tungsten doped ultrathin α-Ni(OH)2 for enhanced electrocatalytic water oxidation. Nature Communications, 2019, 10, 2149.	5.8	363
13	Interstitial Mn ²⁺ -Driven High-Aspect-Ratio Grain Growth for Low-Trap-Density Microcrystalline Films for Record Efficiency CsPbI ₂ Br Solar Cells. ACS Energy Letters, 2018, 3, 970-978.	8.8	356
14	Fabrication of TiO2/C3N4 heterostructure for enhanced photocatalytic Z-scheme overall water splitting. Applied Catalysis B: Environmental, 2016, 191, 130-137.	10.8	344
15	Reducing Detrimental Defects for Highâ€Performance Metal Halide Perovskite Solar Cells. Angewandte Chemie - International Edition, 2020, 59, 6676-6698.	7.2	334
16	One-step hydrothermal synthesis of monolayer MoS ₂ quantum dots for highly efficient electrocatalytic hydrogen evolution. Journal of Materials Chemistry A, 2015, 3, 10693-10697.	5.2	320
17	20â€mmâ€Large Singleâ€Crystalline Formamidiniumâ€Perovskite Wafer for Mass Production of Integrated Photodetectors. Advanced Optical Materials, 2016, 4, 1829-1837.	3.6	316
18	Solution-Processed Nb:SnO ₂ Electron Transport Layer for Efficient Planar Perovskite Solar Cells. ACS Applied Materials & Interfaces, 2017, 9, 2421-2429.	4.0	315

#	Article	IF	CITATIONS
19	Graded Bandgap CsPbl2+Br1â^' Perovskite Solar Cells with a Stabilized Efficiency of 14.4%. Joule, 2018, 2, 1500-1510.	11.7	307
20	3D–2D–0D Interface Profiling for Record Efficiency Allâ€Inorganic CsPbBrl ₂ Perovskite Solar Cells with Superior Stability. Advanced Energy Materials, 2018, 8, 1703246.	10.2	301
21	Thinness―and Shapeâ€Controlled Growth for Ultrathin Singleâ€Crystalline Perovskite Wafers for Mass Production of Superior Photoelectronic Devices. Advanced Materials, 2016, 28, 9204-9209.	11.1	296
22	Polymer Doping for Highâ€Efficiency Perovskite Solar Cells with Improved Moisture Stability. Advanced Energy Materials, 2018, 8, 1701757.	10.2	293
23	Recent Advances in Flexible Perovskite Solar Cells: Fabrication and Applications. Angewandte Chemie - International Edition, 2019, 58, 4466-4483.	7.2	290
24	Nucleation-controlled growth of superior lead-free perovskite Cs3Bi2I9 single-crystals for high-performance X-ray detection. Nature Communications, 2020, 11, 2304.	5.8	286
25	Controlled nâ€Đoping in Air‣table CsPbI ₂ Br Perovskite Solar Cells with a Record Efficiency of 16.79%. Advanced Functional Materials, 2020, 30, 1909972.	7.8	282
26	Highâ€Performance Planar Perovskite Solar Cells Using Low Temperature, Solution–Combustionâ€Based Nickel Oxide Hole Transporting Layer with Efficiency Exceeding 20%. Advanced Energy Materials, 2018, 8, 1703432.	10.2	279
27	Multifunctional Enhancement for Highly Stable and Efficient Perovskite Solar Cells. Advanced Functional Materials, 2021, 31, 2005776.	7.8	273
28	Precursor Engineering for Allâ€Inorganic CsPbI ₂ Br Perovskite Solar Cells with 14.78% Efficiency. Advanced Functional Materials, 2018, 28, 1803269.	7.8	264
29	gâ€C ₃ N ₄ Loading Black Phosphorus Quantum Dot for Efficient and Stable Photocatalytic H ₂ Generation under Visible Light. Advanced Functional Materials, 2018, 28, 1800668.	7.8	257
30	A 1300 mm ² Ultrahighâ€Performance Digital Imaging Assembly using Highâ€Quality Perovskite Single Crystals. Advanced Materials, 2018, 30, e1707314.	11.1	246
31	Phase Transition Control for High Performance Ruddlesden–Popper Perovskite Solar Cells. Advanced Materials, 2018, 30, e1707166.	11.1	244
32	Alkali Metal Doping for Improved CH ₃ NH ₃ PbI ₃ Perovskite Solar Cells. Advanced Science, 2018, 5, 1700131.	5.6	227
33	Recent Progress in Single rystalline Perovskite Research Including Crystal Preparation, Property Evaluation, and Applications. Advanced Science, 2018, 5, 1700471.	5.6	223
34	Energy-Down-Shift CsPbCl ₃ :Mn Quantum Dots for Boosting the Efficiency and Stability of Perovskite Solar Cells. ACS Energy Letters, 2017, 2, 1479-1486.	8.8	221
35	Highâ€Efficiency Perovskite Solar Cells with Imidazoliumâ€Based Ionic Liquid for Surface Passivation and Charge Transport. Angewandte Chemie - International Edition, 2021, 60, 4238-4244.	7.2	221
36	E-beam evaporated Nb2O5 as an effective electron transport layer for large flexible perovskite solar cells. Nano Energy, 2017, 36, 1-8.	8.2	215

#	Article	IF	CITATIONS
37	Multi-inch single-crystalline perovskite membrane for high-detectivity flexible photosensors. Nature Communications, 2018, 9, 5302.	5.8	212
38	Low-temperature-gradient crystallization for multi-inch high-quality perovskite single crystals for record performance photodetectors. Materials Today, 2019, 22, 67-75.	8.3	204
39	Surface-Tension-Controlled Crystallization for High-Quality 2D Perovskite Single Crystals for Ultrahigh Photodetection. Matter, 2019, 1, 465-480.	5.0	202
40	Inch-Size 0D-Structured Lead-Free Perovskite Single Crystals for Highly Sensitive Stable X-Ray Imaging. Matter, 2020, 3, 180-196.	5.0	202
41	µâ€Graphene Crosslinked CsPbI ₃ Quantum Dots for High Efficiency Solar Cells with Much Improved Stability. Advanced Energy Materials, 2018, 8, 1800007.	10.2	198
42	High performance ambient-air-stable FAPbI ₃ perovskite solar cells with molecule-passivated Ruddlesden–Popper/3D heterostructured film. Energy and Environmental Science, 2018, 11, 3358-3366.	15.6	196
43	A review on the stability of inorganic metal halide perovskites: challenges and opportunities for stable solar cells. Energy and Environmental Science, 2021, 14, 2090-2113.	15.6	193
44	Interfaceâ€Modificationâ€Induced Gradient Energy Band for Highly Efficient CsPbIBr ₂ Perovskite Solar Cells. Advanced Energy Materials, 2019, 9, 1803785.	10.2	191
45	Dynamical Transformation of Two-Dimensional Perovskites with Alternating Cations in the Interlayer Space for High-Performance Photovoltaics. Journal of the American Chemical Society, 2019, 141, 2684-2694.	6.6	189
46	Rational Surfaceâ€Defect Control via Designed Passivation for Highâ€Efficiency Inorganic Perovskite Solar Cells. Angewandte Chemie - International Edition, 2021, 60, 23164-23170.	7.2	189
47	Temperature-assisted crystallization for inorganic CsPbI2Br perovskite solar cells to attain high stabilized efficiency 14.81%. Nano Energy, 2018, 52, 408-415.	8.2	186
48	Record‣fficiency Flexible Perovskite Solar Cells Enabled by Multifunctional Organic Ions Interface Passivation. Advanced Materials, 2022, 34, e2201681.	11.1	186
49	Enhancing Efficiency and Stability of Perovskite Solar Cells through Nb-Doping of TiO ₂ at Low Temperature. ACS Applied Materials & Interfaces, 2017, 9, 10752-10758.	4.0	181
50	Progress toward Stable Lead Halide Perovskite Solar Cells. Joule, 2018, 2, 1961-1990.	11.7	181
51	Stable Efficiency Exceeding 20.6% for Inverted Perovskite Solar Cells through Polymer-Optimized PCBM Electron-Transport Layers. Nano Letters, 2019, 19, 3313-3320.	4.5	181
52	Phase Transition Control for High-Performance Blade-Coated Perovskite Solar Cells. Joule, 2018, 2, 1313-1330.	11.7	180
53	Modulating crystal grain size and optoelectronic properties of perovskite films for solar cells by reaction temperature. Nanoscale, 2016, 8, 3816-3822.	2.8	179
54	Design of an Inorganic Mesoporous Holeâ€Transporting Layer for Highly Efficient and Stable Inverted Perovskite Solar Cells. Advanced Materials, 2018, 30, e1805660.	11.1	179

4

#	Article	IF	CITATIONS
55	Fine Multiâ€Phase Alignments in 2D Perovskite Solar Cells with Efficiency over 17% via Slow Postâ€Annealing. Advanced Materials, 2019, 31, e1903889.	11.1	178
56	All-Ambient Processed Binary CsPbBr ₃ –CsPb ₂ Br ₅ Perovskites with Synergistic Enhancement for High-Efficiency Cs–Pb–Br-Based Solar Cells. ACS Applied Materials & Interfaces, 2018, 10, 7145-7154.	4.0	171
57	Compositional Control in 2D Perovskites with Alternating Cations in the Interlayer Space for Photovoltaics with Efficiency over 18%. Advanced Materials, 2019, 31, e1903848.	11.1	171
58	Chlorine doping for black γ-CsPbI3 solar cells with stabilized efficiency beyond 16%. Nano Energy, 2019, 58, 175-182.	8.2	170
59	Telluriumâ€Assisted Epitaxial Growth of Largeâ€Area, Highly Crystalline ReS ₂ Atomic Layers on Mica Substrate. Advanced Materials, 2016, 28, 5019-5024.	11.1	169
60	Superior stability for perovskite solar cells with 20% efficiency using vacuum co-evaporation. Nanoscale, 2017, 9, 12316-12323.	2.8	169
61	A Se-doped MoS ₂ nanosheet for improved hydrogen evolution reaction. Chemical Communications, 2015, 51, 15997-16000.	2.2	167
62	A Novel Anion Doping for Stable CsPbl ₂ Br Perovskite Solar Cells with an Efficiency of 15.56% and an Open Circuit Voltage of 1.30 V. Advanced Energy Materials, 2019, 9, 1902279.	10.2	166
63	Interfacial Engineering at the 2D/3D Heterojunction for High-Performance Perovskite Solar Cells. Nano Letters, 2019, 19, 7181-7190.	4.5	163
64	Tripleâ€Cation and Mixedâ€Halide Perovskite Single Crystal for Highâ€Performance Xâ€ray Imaging. Advanced Materials, 2021, 33, e2006010.	11.1	163
65	Scalable Fabrication of Metal Halide Perovskite Solar Cells and Modules. ACS Energy Letters, 2019, 4, 2147-2167.	8.8	161
66	Printable CsPbI ₃ Perovskite Solar Cells with PCE of 19% via an Additive Strategy. Advanced Materials, 2020, 32, e2001243.	11.1	157
67	2D-MoO ₃ nanosheets for superior gas sensors. Nanoscale, 2016, 8, 8696-8703.	2.8	156
68	NbF ₅ : A Novel αâ€Phase Stabilizer for FAâ€Based Perovskite Solar Cells with High Efficiency. Advanced Functional Materials, 2019, 29, 1807850.	7.8	150
69	Alternating precursor layer deposition for highly stable perovskite films towards efficient solar cells using vacuum deposition. Journal of Materials Chemistry A, 2015, 3, 9401-9405.	5.2	146
70	Waterâ€Soluble Triazolium Ionicâ€Liquidâ€Induced Surface Selfâ€Assembly to Enhance the Stability and Efficiency of Perovskite Solar Cells. Advanced Functional Materials, 2019, 29, 1900417.	7.8	145
71	Highâ€Pressure Nitrogenâ€Extraction and Effective Passivation to Attain Highest Largeâ€Area Perovskite Solar Module Efficiency. Advanced Materials, 2020, 32, e2004979.	11.1	145
72	Efficient planar CsPbBr3 perovskite solar cells by dual-source vacuum evaporation. Solar Energy Materials and Solar Cells, 2018, 187, 1-8.	3.0	139

#	Article	IF	CITATIONS
73	Two-dimensional (PEA) ₂ PbBr ₄ perovskite single crystals for a high performance UV-detector. Journal of Materials Chemistry C, 2019, 7, 1584-1591.	2.7	138
74	Fe(<scp>iii</scp>) doped NiS ₂ nanosheet: a highly efficient and low-cost hydrogen evolution catalyst. Journal of Materials Chemistry A, 2017, 5, 10173-10181.	5.2	137
75	Highly Efficient Ruddlesden–Popper Halide Perovskite PA ₂ MA ₄ Pb ₅ 1 ₁₆ Solar Cells. ACS Energy Letters, 2018, 3, 1975-1982.	8.8	135
76	Interface engineering of low temperature processed all-inorganic CsPbI2Br perovskite solar cells toward PCE exceeding 14%. Nano Energy, 2019, 60, 583-590.	8.2	135
77	Graphdiyne-WS2 2D-Nanohybrid electrocatalysts for high-performance hydrogen evolution reaction. Carbon, 2018, 129, 228-235.	5.4	124
78	Scalable Ambient Fabrication of High-Performance CsPbl2Br Solar Cells. Joule, 2019, 3, 2485-2502.	11.7	124
79	Centimeterâ€Sized Single Crystal of Twoâ€Dimensional Halide Perovskites Incorporating Straightâ€Chain Symmetric Diammonium Ion for Xâ€Ray Detection. Angewandte Chemie - International Edition, 2020, 59, 14896-14902.	7.2	124
80	Molecular Engineering for Two-Dimensional Perovskites with Photovoltaic Efficiency Exceeding 18%. Matter, 2021, 4, 582-599.	5.0	123
81	Polymeric room-temperature molten salt as a multifunctional additive toward highly efficient and stable inverted planar perovskite solar cells. Energy and Environmental Science, 2020, 13, 5068-5079.	15.6	121
82	High-throughput large-area vacuum deposition for high-performance formamidine-based perovskite solar cells. Energy and Environmental Science, 2021, 14, 3035-3043.	15.6	121
83	Perovskite CH ₃ NH ₃ Pb(Br _x I _{1â^`x}) ₃ single crystals with controlled composition for fine-tuned bandgap towards optimized optoelectronic applications. Journal of Materials Chemistry C, 2016, 4, 9172-9178.	2.7	120
84	Room-Temperature Processed Nb ₂ O ₅ as the Electron-Transporting Layer for Efficient Planar Perovskite Solar Cells. ACS Applied Materials & Interfaces, 2017, 9, 23181-23188.	4.0	120
85	Flexible perovskite solar cells with simultaneously improved efficiency, operational stability, and mechanical reliability. Joule, 2021, 5, 1587-1601.	11.7	120
86	Agx@WO3 core-shell nanostructure for LSP enhanced chemical sensors. Scientific Reports, 2014, 4, 6745.	1.6	116
87	CsPb(I Br1â^')3 solar cells. Science Bulletin, 2019, 64, 1532-1539.	4.3	114
88	Photoelectrochemical CO ₂ reduction to adjustable syngas on grain-boundary-mediated a-Si/TiO ₂ /Au photocathodes with low onset potentials. Energy and Environmental Science, 2019, 12, 923-928.	15.6	114
89	Nitrogen-doped graphene quantum dots for 80% photoluminescence quantum yield for inorganic γ-CsPbl ₃ perovskite solar cells with efficiency beyond 16%. Journal of Materials Chemistry A, 2019, 7, 5740-5747.	5.2	113
90	Ruddlesden–Popper 2D Component to Stabilize γ sPbI ₃ Perovskite Phase for Stable and Efficient Photovoltaics. Advanced Energy Materials, 2019, 9, 1902529.	10.2	111

#	Article	IF	CITATIONS
91	40.1% Record Lowâ€Light Solarâ€Cell Efficiency by Holistic Trapâ€Passivation using Micrometerâ€Thick Perovskite Film. Advanced Materials, 2021, 33, e2100770.	11.1	110
92	Gas-solid reaction based over one-micrometer thick stable perovskite films for efficient solar cells and modules. Nature Communications, 2018, 9, 3880.	5.8	109
93	Synthesis of Largeâ€Size 1T′ ReS ₂ <i>_x</i> Se _{2(1â^'} <i>_x</i> ₎ Alloy Monolayer with Tunable Bandgap and Carrier Type. Advanced Materials, 2017, 29, 1705015.	11.1	107
94	120 mm single-crystalline perovskite and wafers: towards viable applications. Science China Chemistry, 2017, 60, 1367-1376.	4.2	107
95	Color-Tuned Perovskite Films Prepared for Efficient Solar Cell Applications. Journal of Physical Chemistry C, 2016, 120, 42-47.	1.5	106
96	Precursor Engineering for Ambientâ€Compatible Antisolventâ€Free Fabrication of Highâ€Efficiency CsPbl ₂ Br Perovskite Solar Cells. Advanced Energy Materials, 2020, 10, 2000691.	10.2	106
97	2D Cs ₂ Pbl ₂ Cl ₂ Nanosheets for Holistic Passivation of Inorganic CsPbl ₂ Br Perovskite Solar Cells for Improved Efficiency and Stability. Advanced Energy Materials, 2020, 10, 2002882.	10.2	105
98	ITIC surface modification to achieve synergistic electron transport layer enhancement for planar-type perovskite solar cells with efficiency exceeding 20%. Journal of Materials Chemistry A, 2017, 5, 9514-9522.	5.2	103
99	One-pot hydrothermal fabrication of layered \hat{l}^2 -Ni(OH) 2 /g-C 3 N 4 nanohybrids for enhanced photocatalytic water splitting. Applied Catalysis B: Environmental, 2016, 194, 74-83.	10.8	102
100	High Density and Unit Activity Integrated in Amorphous Catalysts for Electrochemical Water Splitting. Small Structures, 2021, 2, 2000096.	6.9	102
101	Pt monolayer coating on complex network substrate with high catalytic activity for the hydrogen evolution reaction. Science Advances, 2015, 1, e1400268.	4.7	97
102	Improve the oxide/perovskite heterojunction contact for low temperature high efficiency and stable all-inorganic CsPbI2Br perovskite solar cells. Nano Energy, 2020, 67, 104241.	8.2	97
103	Unveiling the Effects of Hydrolysisâ€Derived DMAI/DMAPbI <i>_x</i> Intermediate Compound on the Performance of CsPbI ₃ Solar Cells. Advanced Science, 2020, 7, 1902868.	5.6	97
104	Ionic Liquid Treatment for Highestâ€Efficiency Ambient Printed Stable Allâ€Inorganic CsPbI ₃ Perovskite Solar Cells. Advanced Materials, 2022, 34, e2106750.	11.1	97
105	Low Temperature Fabrication for High Performance Flexible CsPbl ₂ Br Perovskite Solar Cells. Advanced Science, 2018, 5, 1801117.	5.6	96
106	Polar rotor scattering as atomic-level origin of low mobility and thermal conductivity of perovskite CH3NH3PbI3. Nature Communications, 2017, 8, 16086.	5.8	95
107	Europium and Acetate Coâ€doping Strategy for Developing Stable and Efficient CsPbI ₂ Br Perovskite Solar Cells. Small, 2019, 15, e1904387.	5.2	95
108	Hydrazide Derivatives for Defect Passivation in Pure CsPbI ₃ Perovskite Solar Cells. Angewandte Chemie - International Edition, 2022, 61, .	7.2	95

#	Article	IF	CITATIONS
109	Large and Dense Organic–Inorganic Hybrid Perovskite CH ₃ NH ₃ PbI ₃ Wafer Fabricated by One-Step Reactive Direct Wafer Production with High X-ray Sensitivity. ACS Applied Materials & Interfaces, 2020, 12, 16592-16600.	4.0	94
110	Stable ultra-fast broad-bandwidth photodetectors based on α-CsPbI ₃ perovskite and NaYF ₄ :Yb,Er quantum dots. Nanoscale, 2017, 9, 6278-6285.	2.8	93
111	Additive Engineering to Grow Micronâ€Sized Grains for Stable High Efficiency Perovskite Solar Cells. Advanced Science, 2019, 6, 1901241.	5.6	93
112	Goldschmidt-rule-deviated perovskite CsPbIBr2by barium substitution for efficient solar cells. Nano Energy, 2019, 61, 165-172.	8.2	93
113	28.3%-efficiency perovskite/silicon tandem solar cell by optimal transparent electrode for high efficient semitransparent top cell. Nano Energy, 2021, 84, 105934.	8.2	93
114	High-Performance, Self-Powered Photodetectors Based on Perovskite and Graphene. ACS Applied Materials & Interfaces, 2017, 9, 42779-42787.	4.0	91
115	27%â€Efficiency Fourâ€Terminal Perovskite/Silicon Tandem Solar Cells by Sandwiched Gold Nanomesh. Advanced Functional Materials, 2020, 30, 1908298.	7.8	91
116	Ag Nanoparticle-Sensitized WO ₃ Hollow Nanosphere for Localized Surface Plasmon Enhanced Gas Sensors. ACS Applied Materials & Interfaces, 2016, 8, 18165-18172.	4.0	90
117	High-performance transparent ultraviolet photodetectors based on inorganic perovskite CsPbCl ₃ nanocrystals. RSC Advances, 2017, 7, 36722-36727.	1.7	90
118	Iodineâ€Optimized Interface for Inorganic CsPbl ₂ Br Perovskite Solar Cell to Attain High Stabilized Efficiency Exceeding 14%. Advanced Science, 2018, 5, 1801123.	5.6	90
119	Thermally stable methylammonium-free inverted perovskite solar cells with Zn2+ doped CuGaO2 as efficient mesoporous hole-transporting layer. Nano Energy, 2019, 61, 148-157.	8.2	90
120	In Situ Synthesis of Fewâ€Layered gâ€C ₃ N ₄ with Vertically Aligned MoS ₂ Loading for Boosting Solarâ€toâ€Hydrogen Generation. Small, 2018, 14, 1703003.	5.2	90
121	P Doped MoO _{3â^'} <i>_x</i> Nanosheets as Efficient and Stable Electrocatalysts for Hydrogen Evolution. Small, 2017, 13, 1700441.	5.2	88
122	Graphene-oxide doped PEDOT:PSS as a superior hole transport material for high-efficiency perovskite solar cell. Organic Electronics, 2017, 48, 165-171.	1.4	87
123	Vapor-fumigation for record efficiency two-dimensional perovskite solar cells with superior stability. Energy and Environmental Science, 2018, 11, 3349-3357.	15.6	87
124	Highly Efficient and Stable Planar Perovskite Solar Cells with Modulated Diffusion Passivation Toward High Power Conversion Efficiency and Ultrahigh Fill Factor. Solar Rrl, 2019, 3, 1900293.	3.1	87
125	A Special Additive Enables All Cations and Anions Passivation for Stable Perovskite Solar Cells with Efficiency over 23%. Nano-Micro Letters, 2021, 13, 169.	14.4	86
126	Novel inorganic electron transport layers for planar perovskite solar cells: Progress and prospective. Nano Energy, 2020, 68, 104289.	8.2	83

Shengzhong Frank Liu

#	Article	IF	CITATIONS
127	WO 3 -SnO 2 nanosheet composites: Hydrothermal synthesis and gas sensing mechanism. Journal of Alloys and Compounds, 2018, 736, 322-331.	2.8	82
128	Bifunctional Hydroxylamine Hydrochloride Incorporated Perovskite Films for Efficient and Stable Planar Perovskite Solar Cells. ACS Applied Energy Materials, 2018, 1, 900-909.	2.5	81
129	Inch-sized high-quality perovskite single crystals by suppressing phase segregation for light-powered integrated circuits. Science Advances, 2021, 7, .	4.7	81
130	Moltenâ€Saltâ€Assisted CsPbI ₃ Perovskite Crystallization for Nearly 20%â€Efficiency Solar Cells. Advanced Materials, 2021, 33, e2103770.	11.1	81
131	Perovskite—a Perfect Top Cell for Tandem Devices to Break the S–Q Limit. Advanced Science, 2019, 6, 1801704.	5.6	80
132	Recent progress of twoâ€dimensional lead halide perovskite single crystals: Crystal growth, physical properties, and device applications. EcoMat, 2020, 2, e12036.	6.8	80
133	Ionicâ€Liquidâ€Perovskite Capping Layer for Stable 24.33%â€Efficient Solar Cell. Advanced Energy Materials, 2022, 12, .	10.2	80
134	An up-scalable approach to CH3NH3PbI3 compact films for high-performance perovskite solar cells. Nano Energy, 2015, 15, 670-678.	8.2	79
135	Defect Engineering in Earthâ€Abundant Cu ₂ ZnSn(S,Se) ₄ Photovoltaic Materials via Ga ³⁺ â€Doping for over 12% Efficient Solar Cells. Advanced Functional Materials, 2021, 31, 2010325.	7.8	79
136	Low-temperature and facile solution-processed two-dimensional TiS ₂ as an effective electron transport layer for UV-stable planar perovskite solar cells. Journal of Materials Chemistry A, 2018, 6, 9132-9138.	5.2	78
137	Stability of the CsPbI ₃ perovskite: from fundamentals to improvements. Journal of Materials Chemistry A, 2021, 9, 11124-11144.	5.2	78
138	Recent Advances in Photoelectrochemical Applications of Silicon Materials for Solarâ€toâ€Chemicals Conversion. ChemSusChem, 2017, 10, 4324-4341.	3.6	77
139	Graphdiyne Quantum Dots for Much Improved Stability and Efficiency of Perovskite Solar Cells. Advanced Materials Interfaces, 2018, 5, 1701117.	1.9	76
140	High-quality perovskite MAPbI3 single crystals for broad-spectrum and rapid response integrate photodetector. Journal of Energy Chemistry, 2018, 27, 722-727.	7.1	76
141	Cesium Lead Mixed-Halide Perovskites for Low-Energy Loss Solar Cells with Efficiency Beyond 17%. Chemistry of Materials, 2019, 31, 6231-6238.	3.2	76
142	Highâ€Efficiency Perovskite Solar Cells Enabled by Anatase TiO ₂ Nanopyramid Arrays with an Oriented Electric Field. Angewandte Chemie - International Edition, 2020, 59, 11969-11976.	7.2	76
143	Zn-doping for reduced hysteresis and improved performance of methylammonium lead iodide perovskite hybrid solar cells. Materials Today Energy, 2017, 5, 205-213.	2.5	75
144	Ultrastable Perovskite–Zeolite Composite Enabled by Encapsulation and Inâ€Situ Passivation. Angewandte Chemie - International Edition, 2020, 59, 23100-23106.	7.2	75

#	Article	IF	CITATIONS
145	Simultaneous Cesium and Acetate Coalloying Improves Efficiency and Stability of FA _{0.85} MA _{0.15} PbI ₃ Perovskite Solar Cell with an Efficiency of 21.95%. Solar Rrl, 2019, 3, 1900220.	3.1	74
146	Dual Passivation of Perovskite and SnO ₂ for Highâ€Efficiency MAPbI ₃ Perovskite Solar Cells. Advanced Science, 2021, 8, 2001466.	5.6	72
147	Synthesis and formation mechanism of flowerlike architectures assembled from ultrathin NiO nanoflakes and their adsorption to malachite green and acid red in water. Chemical Engineering Journal, 2014, 239, 141-148.	6.6	71
148	Metal Cations in Efficient Perovskite Solar Cells: Progress and Perspective. Advanced Materials, 2019, 31, e1902037.	11.1	71
149	<i>>m</i> -Phenylenediammonium as a New Spacer for Dion–Jacobson Two-Dimensional Perovskites. Journal of the American Chemical Society, 2021, 143, 12063-12073.	6.6	71
150	Stable High-Performance Flexible Photodetector Based on Upconversion Nanoparticles/Perovskite Microarrays Composite. ACS Applied Materials & Interfaces, 2017, 9, 19176-19183.	4.0	70
151	Recent advances in resistive random access memory based on lead halide perovskite. InformaÄnÃ- Materiály, 2021, 3, 293-315.	8.5	70
152	Epitaxial growth of large-area and highly crystalline anisotropic ReSe2 atomic layer. Nano Research, 2017, 10, 2732-2742.	5.8	69
153	Interfaces and Interfacial Layers in Inorganic Perovskite Solar Cells. Angewandte Chemie - International Edition, 2021, 60, 26440-26453.	7.2	69
154	Preparation of ZnO hollow spheres with different surface roughness and their enhanced gas sensing property. Sensors and Actuators B: Chemical, 2014, 197, 58-65.	4.0	68
155	Path towards high-efficient kesterite solar cells. Journal of Energy Chemistry, 2018, 27, 1040-1053.	7.1	68
156	Synergy of Hydrophobic Surface Capping and Lattice Contraction for Stable and Highâ€Efficiency Inorganic CsPbI ₂ Br Perovskite Solar Cells. Solar Rrl, 2018, 2, 1800216.	3.1	68
157	Ambient blade coating of mixed cation, mixed halide perovskites without dripping: <i>in situ</i> investigation and highly efficient solar cells. Journal of Materials Chemistry A, 2020, 8, 1095-1104.	5.2	68
158	Metalâ€Free Halide Perovskite Single Crystals with Very Long Charge Lifetimes for Efficient Xâ€ray Imaging. Advanced Materials, 2020, 32, e2003353.	11.1	68
159	Efficient perovskite solar cells <i>via</i> surface passivation by a multifunctional small organic ionic compound. Journal of Materials Chemistry A, 2020, 8, 8313-8322.	5.2	68
160	Recent Progress of Electrode Materials for Flexible Perovskite Solar Cells. Nano-Micro Letters, 2022, 14, 117.	14.4	68
161	Heterojunction CuO@ZnO microcubes for superior p-type gas sensor application. Journal of Alloys and Compounds, 2016, 672, 374-379.	2.8	67
162	Large Leadâ€Free Perovskite Single Crystal for Highâ€Performance Coplanar Xâ€Ray Imaging Applications. Advanced Optical Materials, 2020, 8, 2000814.	3.6	67

#	Article	IF	CITATIONS
163	Lowâ€Temperature Solutionâ€Processed ZnO Electron Transport Layer for Highly Efficient and Stable Planar Perovskite Solar Cells with Efficiency Over 20%. Solar Rrl, 2019, 3, 1900096.	3.1	66
164	Enhanced Efficiency and Stability of Allâ€Inorganic CsPbI ₂ Br Perovskite Solar Cells by Organic and Ionic Mixed Passivation. Advanced Science, 2021, 8, e2101367.	5.6	66
165	CsPbCl ₃ â€Driven Lowâ€Trapâ€Density Perovskite Grain Growth for >20% Solar Cell Efficiency. Advanced Science, 2018, 5, 1800474.	5.6	65
166	Novel Surface Passivation for Stable FA _{0.85} MA _{0.15} PbI ₃ Perovskite Solar Cells with 21.6% Efficiency. Solar Rrl, 2019, 3, 1900072.	3.1	64
167	Metal-doped Mo2C (metal = Fe, Co, Ni, Cu) as catalysts on TiO2 for photocatalytic hydrogen evolution in neutral solution. Chinese Journal of Catalysis, 2021, 42, 205-216.	6.9	64
168	Film Formation Control for High Performance Dion–Jacobson 2D Perovskite Solar Cells. Advanced Energy Materials, 2021, 11, 2002733.	10.2	62
169	Fe ₂ O ₃ /C–C ₃ N ₄ -Based Tight Heterojunction for Boosting Visible-Light-Driven Photocatalytic Water Oxidation. ACS Sustainable Chemistry and Engineering, 2018, 6, 10436-10444.	3.2	61
170	Improved PEDOT:PSS/c-Si hybrid solar cell using inverted structure and effective passivation. Scientific Reports, 2016, 6, 35091.	1.6	60
171	Interface engineering of CsPbBr3/TiO2 heterostructure with enhanced optoelectronic properties for all-inorganic perovskite solar cells. Applied Physics Letters, 2018, 112, .	1.5	60
172	Intermediate phase engineering of halide perovskites for photovoltaics. Joule, 2022, 6, 315-339.	11.7	60
173	Wideâ€Bandgap Organic–Inorganic Lead Halide Perovskite Solar Cells. Advanced Science, 2022, 9, e2105085.	5.6	60
174	Direct growth of ZnO nanodisk networks with an exposed (0001) facet on Au comb-shaped interdigitating electrodes and the enhanced gas-sensing property of polar {0001} surfaces. Sensors and Actuators B: Chemical, 2014, 195, 71-79.	4.0	59
175	Organic–Inorganic Hybrid Perovskite with Controlled Dopant Modification and Application in Photovoltaic Device. Small, 2017, 13, 1604153.	5.2	59
176	A High Mobility Conjugated Polymer Enables Air and Thermally Stable CsPbI ₂ Br Perovskite Solar Cells with an Efficiency Exceeding 15%. Advanced Materials Technologies, 2019, 4, 1900311.	3.0	59
177	Air and thermally stable perovskite solar cells with CVD-graphene as the blocking layer. Nanoscale, 2017, 9, 8274-8280.	2.8	58
178	Synthesis of thickness-controlled cuboid WO3 nanosheets and their exposed facets-dependent acetone sensing properties. Journal of Alloys and Compounds, 2017, 696, 490-497.	2.8	58
179	Optical Management with Nanoparticles for a Light Conversion Efficiency Enhancement in Inorganic γ-CsPbI ₃ Solar Cells. Nano Letters, 2019, 19, 1796-1804.	4.5	58
180	Fabrication of efficient CsPbBr3 perovskite solar cells by single-source thermal evaporation. Journal of Alloys and Compounds, 2020, 818, 152903.	2.8	58

#	Article	IF	CITATIONS
181	Rational Surfaceâ€Defect Control via Designed Passivation for Highâ€Efficiency Inorganic Perovskite Solar Cells. Angewandte Chemie, 2021, 133, 23348-23354.	1.6	58
182	Unraveling Passivation Mechanism of Imidazolium-Based Ionic Liquids on Inorganic Perovskite to Achieve Near-Record-Efficiency CsPbI2Br Solar Cells. Nano-Micro Letters, 2022, 14, 7.	14.4	58
183	One-pot fabrication of NiFe 2 O 4 nanoparticles on α-Ni(OH) 2 nanosheet for enhanced water oxidation. Journal of Power Sources, 2016, 324, 499-508.	4.0	57
184	2D Perovskite Single Crystals with Suppressed Ion Migration for Highâ€Performance Planarâ€Type Photodetectors. Small, 2020, 16, e2003145.	5.2	56
185	Mn Doping of CsPbl ₃ Film Towards High-Efficiency Solar Cell. ACS Applied Energy Materials, 2020, 3, 5190-5197.	2.5	56
186	Flexible perovskite solar cells based on green, continuous roll-to-roll printing technology. Journal of Energy Chemistry, 2018, 27, 971-989.	7.1	55
187	Earth-abundant elements doping for robust and stable solar-driven water splitting by FeOOH. Journal of Materials Chemistry A, 2017, 5, 21478-21485.	5.2	54
188	The humidity-insensitive fabrication of efficient CsPbI ₃ solar cells in ambient air. Journal of Materials Chemistry A, 2019, 7, 26776-26784.	5.2	54
189	Stable 24.29%â€Efficiency FA _{0.85} MA _{0.15} PbI ₃ Perovskite Solar Cells Enabled by Methyl Haloacetateâ€Lead Dimer Complex. Advanced Energy Materials, 2022, 12, .	10.2	54
190	Pseudohalide (SCN ^{â^'})-doped CsPbI ₃ for high-performance solar cells. Journal of Materials Chemistry C, 2019, 7, 13736-13742.	2.7	53
191	Two dimensional metal halide perovskites: Promising candidates for light-emitting diodes. Journal of Energy Chemistry, 2019, 37, 97-110.	7.1	52
192	Record‣owâ€Threshold Lasers Based on Atomically Smooth Triangular Nanoplatelet Perovskite. Advanced Functional Materials, 2019, 29, 1805553.	7.8	52
193	Superior adsorption performance for triphenylmethane dyes on 3D architectures assembled by ZnO nanosheets as thin as â^1/41.5 nm. Journal of Hazardous Materials, 2016, 318, 732-741.	6.5	51
194	Breaking Platinum Nanoparticles to Singleâ€Atomic Ptâ€C ₄ Coâ€catalysts for Enhanced Solarâ€toâ€Hydrogen Conversion. Angewandte Chemie - International Edition, 2021, 60, 2541-2547.	7.2	51
195	Facile synthesis of an iron doped rutile TiO ₂ photocatalyst for enhanced visible-light-driven water oxidation. Journal of Materials Chemistry A, 2015, 3, 21434-21438.	5.2	50
196	Enhancing the Sensing Properties of TiO ₂ Nanosheets with Exposed {001} Facets by a Hydrogenation and Sensing Mechanism. Inorganic Chemistry, 2017, 56, 1504-1510.	1.9	50
197	Anti-solvent engineering for efficient semitransparent CH3NH3PbBr3 perovskite solar cells for greenhouse applications. Journal of Energy Chemistry, 2019, 34, 12-19.	7.1	50
198	Fluoroethylamine Engineering for Effective Passivation to Attain 23.4% Efficiency Perovskite Solar Cells with Superior Stability. Advanced Energy Materials, 2021, 11, 2101454.	10.2	49

#	Article	IF	CITATIONS
199	Nâ€Type Surface Design for pâ€Type CZTSSe Thin Film to Attain High Efficiency. Advanced Materials, 2021, 33, e2104330.	11.1	49
200	Perovskite Quantum Dots in Solar Cells. Advanced Science, 2022, 9, e2104577.	5.6	49
201	Chlorineâ€modified SnO ₂ electron transport layer for highâ€efficiency perovskite solar cells. InformaÄnÃ-Materiály, 2020, 2, 401-408.	8.5	48
202	Solvent Engineering Using a Volatile Solid for Highly Efficient and Stable Perovskite Solar Cells. Advanced Science, 2020, 7, 1903250.	5.6	47
203	Antisolvent―and Annealingâ€Free Deposition for Highly Stable Efficient Perovskite Solar Cells via Modified ZnO. Advanced Science, 2021, 8, 2002860.	5.6	47
204	Halide-modulated self-assembly of metal-free perovskite single crystals for bio-friendly X-ray detection. Matter, 2021, 4, 2490-2507.	5.0	47
205	Symmetrical Acceptor–Donor–Acceptor Molecule as a Versatile Defect Passivation Agent toward Efficient FA _{0.85} MA _{0.15} Pbl ₃ Perovskite Solar Cells. Advanced Functional Materials, 2022, 32, .	7.8	47
206	One-step preparation of optically transparent Ni-Fe oxide film electrocatalyst for oxygen evolution reaction. Electrochimica Acta, 2015, 169, 402-408.	2.6	46
207	Dual interfacial engineering for efficient Cs2AgBiBr6 based solar cells. Journal of Energy Chemistry, 2021, 53, 372-378.	7.1	46
208	Highly Luminescent Metalâ€Free Perovskite Single Crystal for Biocompatible Xâ€Ray Detector to Attain Highest Sensitivity. Advanced Materials, 2021, 33, e2102190.	11.1	46
209	2D WS2 nanosheet supported Pt nanoparticles for enhanced hydrogen evolution reaction. International Journal of Hydrogen Energy, 2017, 42, 5472-5477.	3.8	45
210	Synthesis of Ag quantum dots sensitized WO3 nanosheets and their enhanced acetone sensing properties. Materials Letters, 2017, 186, 66-69.	1.3	45
211	Highly efficient and stable planar CsPbi2Br perovskite solar cell with a new sensitive-dopant-free hole transport layer obtained via an effective surface passivation. Solar Energy Materials and Solar Cells, 2019, 201, 110052.	3.0	45
212	Layer-Dependent Ultrahigh-Mobility Transport Properties in All-Inorganic Two-Dimensional Cs ₂ PbI ₂ Cl ₂ and Cs ₂ SnI ₂ Cl ₂ Perovskites. Journal of Physical Chemistry C, 2019, 123, 27978-27985.	1.5	45
213	Impact of the Solvation State of Lead Iodide on Its Twoâ€Step Conversion to MAPbI ₃ : An In Situ Investigation. Advanced Functional Materials, 2019, 29, 1807544.	7.8	45
214	Increasing Quantum Efficiency of Polymer Solar Cells with Efficient Exciton Splitting and Long Carrier Lifetime by Molecular Doping at Heterojunctions. ACS Energy Letters, 2019, 4, 1356-1363.	8.8	45
215	Enhanced Efficiency of Inorganic CsPbI _{3â^'} <i>_x</i> Br <i>_x</i> Perovskite Solar Cell via Selfâ€Regulation of Antisite Defects. Advanced Energy Materials, 2021, 11, 2100403.	10.2	45
216	Stable 2D Alternating Cation Perovskite Solar Cells with Power Conversion Efficiency >19% via Solvent Engineering. Solar Rrl, 2021, 5, 2100286.	3.1	45

#	Article	IF	CITATIONS
217	Development of an alcohol sensor based on ZnO nanorods synthesized using a scalable solvothermal method. Sensors and Actuators B: Chemical, 2013, 185, 735-742.	4.0	44
218	Extrinsic Ion Distribution Induced Field Effect in CsPbIBr ₂ Perovskite Solar Cells. Small, 2020, 16, e1907283.	5.2	44
219	A Key 2D Intermediate Phase for Stable Highâ€Efficiency CsPbI ₂ Br Perovskite Solar Cells. Advanced Energy Materials, 2022, 12, 2103019.	10.2	44
220	Powering the World with Solar Fuels from Photoelectrochemical CO ₂ Reduction: Basic Principles and Recent Advances. Advanced Energy Materials, 2022, 12, .	10.2	44
221	Visible-light photocatalysis in Cu ₂ Se nanowires with exposed {111} facets and charge separation between (111) and (1Ì,,1Ì,,1Ì,) polar surfaces. Physical Chemistry Chemical Physics, 2015, 17, 13280-13289.	1.3	42
222	First-Principles Study of Enhanced Out-of-Plane Transport Properties and Stability in Dion–Jacobson Two-Dimensional Perovskite Semiconductors for High-Performance Solar Cell Applications. Journal of Physical Chemistry Letters, 2019, 10, 3670-3675.	2.1	42
223	Inâ€5itu Hot Oxygen Cleansing and Passivation for Allâ€Inorganic Perovskite Solar Cells Deposited in Ambient to Breakthrough 19% Efficiency. Advanced Functional Materials, 2021, 31, 2101568.	7.8	42
224	Green antisolvent additive engineering to improve the performance of perovskite solar cells. Journal of Energy Chemistry, 2022, 66, 1-8.	7.1	42
225	Spontaneous Construction of Multidimensional Heterostructure Enables Enhanced Hole Extraction for Inorganic Perovskite Solar Cells to Exceed 20% Efficiency. Advanced Energy Materials, 2022, 12, 2103007.	10.2	42
226	Superior photocatalytic activities of NiO octahedrons with loaded AgCl particles and charge separation between polar NiO {111} surfaces. Applied Catalysis B: Environmental, 2015, 172-173, 165-173.	10.8	41
227	Controlled defects and enhanced electronic extraction in fluorine-incorporated zinc oxide for high-performance planar perovskite solar cells. Solar Energy Materials and Solar Cells, 2018, 182, 263-271.	3.0	41
228	Roomâ€Temperature Partial Conversion of αâ€FAPbI ₃ Perovskite Phase via PbI ₂ Solvation Enables Highâ€Performance Solar Cells. Advanced Functional Materials, 2020, 30, 1907442.	7.8	41
229	Samariumâ€Doped Nickel Oxide for Superior Inverted Perovskite Solar Cells: Insight into Doping Effect for Electronic Applications. Advanced Functional Materials, 2021, 31, 2102452.	7.8	41
230	Topology and texture controlled ZnO thin film electrodeposition for superior solar cell efficiency. Solar Energy Materials and Solar Cells, 2015, 134, 54-59.	3.0	40
231	MoS 2 /sulfur and nitrogen co-doped reduced graphene oxide nanocomposite for enhanced electrocatalytic hydrogen evolution. International Journal of Hydrogen Energy, 2016, 41, 916-923.	3.8	40
232	Enhanced luminescence and tunable color of Sr8CaSc(PO4)7:Eu2+, Ce3+, Mn2+ phosphor by energy transfer between Ce3+-Eu2+-Mn2+. Journal of Alloys and Compounds, 2018, 731, 796-804.	2.8	40
233	2D–3D Cs ₂ PbI ₂ Cl ₂ –CsPbI _{2.5} Br _{0.5} Mixed-Dimensional Films for All-Inorganic Perovskite Solar Cells with Enhanced Efficiency and Stability. Journal of Physical Chemistry Letters, 2020, 11, 4138-4146.	2.1	40
234	Recent Developments in Upscalable Printing Techniques for Perovskite Solar Cells. Advanced Science, 2022, 9, e2200308.	5.6	40

#	Article	IF	CITATIONS
235	Responses of three-dimensional porous ZnO foam structures to the trace level of triethylamine and ethanol. Sensors and Actuators B: Chemical, 2016, 223, 650-657.	4.0	39
236	Photo-Redeposition Synthesis of Bimetal Pt–Cu Co-catalysts for TiO ₂ Photocatalytic Solar-Fuel Production. ACS Sustainable Chemistry and Engineering, 2020, 8, 6055-6064.	3.2	39
237	Ligand-Size Related Dimensionality Control in Metal Halide Perovskites. ACS Energy Letters, 2019, 4, 1830-1838.	8.8	38
238	Ligandâ€Anchoringâ€Induced Oriented Crystal Growth for Highâ€Efficiency Leadâ€Tin Perovskite Solar Cells. Advanced Functional Materials, 2022, 32, .	7.8	38
239	Quasiâ€Amorphous Metallic Nickel Nanopowder as an Efficient and Durable Electrocatalyst for Alkaline Hydrogen Evolution. Advanced Science, 2018, 5, 1801216.	5.6	37
240	Zero-thermal-quenching and photoluminescence tuning with the assistance of carriers from defect cluster traps. Journal of Materials Chemistry C, 2018, 6, 10687-10692.	2.7	37
241	Defects in CsPbX ₃ Perovskite: From Understanding to Effective Manipulation for Highâ€Performance Solar Cells. Small Methods, 2021, 5, e2100725.	4.6	37
242	Synergistic Crystallization and Passivation by a Single Molecular Additive for Highâ€₽erformance Perovskite Solar Cells. Advanced Materials, 2022, 34, .	11.1	37
243	Effective light trapping by hybrid nanostructure for crystalline silicon solar cells. Solar Energy Materials and Solar Cells, 2015, 140, 180-186.	3.0	36
244	Influence of oxygen pressure on the structural and electrical properties of CuO thin films prepared by pulsed laser deposition. Materials Letters, 2016, 176, 282-284.	1.3	36
245	Air-stable phosphorus-doped molybdenum nitride for enhanced electrocatalytic hydrogen evolution. Communications Chemistry, 2018, 1, .	2.0	36
246	Chemical Bath Deposition of Coâ€Doped TiO ₂ Electron Transport Layer for Hysteresisâ€Suppressed Highâ€Efficiency Planar Perovskite Solar Cells. Solar Rrl, 2019, 3, 1900176.	3.1	36
247	Defect suppression in multinary chalcogenide photovoltaic materials derived from kesterite: progress and outlook. Journal of Materials Chemistry A, 2020, 8, 24920-24942.	5.2	36
248	Firstâ€Principles Calculation Design for 2D Perovskite to Suppress Ion Migration for Highâ€Performance Xâ€ray Detection. Advanced Functional Materials, 2022, 32, .	7.8	36
249	Synthesis of CuO microstructures with controlled shape and size and their exposed facets induced enhanced ethanol sensing performance. Sensors and Actuators B: Chemical, 2016, 227, 328-335.	4.0	35
250	Controllable synthesis of Ag-WO3 core-shell nanospheres for light-enhanced gas sensors. Sensors and Actuators B: Chemical, 2017, 251, 583-589.	4.0	35
251	CO ₂ Plasma-Treated TiO ₂ Film as an Effective Electron Transport Layer for High-Performance Planar Perovskite Solar Cells. ACS Applied Materials & Interfaces, 2017, 9, 33989-33996.	4.0	35
252	Realizing efficient red thermally activated delayed fluorescence organic light-emitting diodes using phenoxazine/phenothiazine-phenanthrene hybrids. Organic Electronics, 2018, 59, 32-38.	1.4	35

#	Article	IF	CITATIONS
253	Unveiling the effect of interstitial dopants on CO2 activation over CsPbBr3 catalyst for efficient photothermal CO2 reduction. Chemical Engineering Journal, 2022, 435, 135071.	6.6	35
254	Surface reconstruction strategy improves the all-inorganic CsPbIBr2 based perovskite solar cells and photodetectors performance. Nano Energy, 2022, 94, 106960.	8.2	35
255	Li doping effect on the photoluminescence behaviors of KSrPO4:Dy3+ phosphors for WLED light. Materials Research Bulletin, 2015, 64, 364-369.	2.7	34
256	Superior sensor performance from Ag@WO3 core–shell nanostructure. Journal of Alloys and Compounds, 2015, 623, 127-131.	2.8	34
257	Solution Coating of Superior Largeâ€Area Flexible Perovskite Thin Films with Controlled Crystal Packing. Advanced Optical Materials, 2017, 5, 1700102.	3.6	34
258	Nitrogen-promoted molybdenum dioxide nanosheets for electrochemical hydrogen generation. Journal of Materials Chemistry A, 2018, 6, 12532-12540.	5.2	34
259	Fabrication of nanoporous Ni and NiO via a dealloying strategy for water oxidation catalysis. Journal of Energy Chemistry, 2020, 50, 125-134.	7.1	34
260	pâ€Type Carbon Dots for Effective Surface Optimization for Nearâ€Recordâ€Efficiency CsPbl ₂ Br Solar Cells. Small, 2021, 17, e2102272.	5.2	34
261	Graded 2D/3D (CF3-PEA)2FA0.85MA0.15Pb2I7/FA0.85MA0.15PbI3 heterojunction for stable perovskite solar cell with an efficiency over 23.0%. Journal of Energy Chemistry, 2022, 65, 480-489.	7.1	34
262	Single-crystalline lead halide perovskite wafers for high performance photodetectors. Journal of Materials Chemistry C, 2019, 7, 8357-8363.	2.7	33
263	Composition controlled preparation of Cu–Zn–Sn precursor films for Cu2ZnSnS4 solar cells using pulsed electrodeposition. Journal of Alloys and Compounds, 2015, 650, 1-7.	2.8	32
264	Effective Phaseâ€Alignment for 2D Halide Perovskites Incorporating Symmetric Diammonium Ion for Photovoltaics. Advanced Science, 2021, 8, e2001433.	5.6	32
265	Controlled ZnO hierarchical structure for improved gas sensing performance. Sensors and Actuators B: Chemical, 2015, 209, 343-351.	4.0	31
266	Kesterite Cu ₂ Zn(Sn,Ge)(S,Se) ₄ thin film with controlled Ge-doping for photovoltaic application. Nanoscale, 2016, 8, 10160-10165.	2.8	31
267	Hydrogenated nanotubes/nanowires assembled from TiO ₂ nanoflakes with exposed {111} facets: excellent photo-catalytic CO ₂ reduction activity and charge separation mechanism between (111) and (1Ì,,1Ì,,1Ì,,) polar surfaces. Journal of Materials Chemistry A, 2019, 7, 14761-14775.	5.2	31
268	Lowâ€Temperature Crystallization of CsPbIBr ₂ Perovskite for High Performance Solar Cells. Solar Rrl, 2020, 4, 2000254.	3.1	31
269	In Situ Study of Molecular Aggregation in Conjugated Polymer/Elastomer Blends toward Stretchable Electronics. Macromolecules, 2022, 55, 297-308.	2.2	30
270	Deepâ€Ultraviolet Photoactivationâ€Assisted Contact Engineering Toward Highâ€Efficiency and Stable Allâ€Inorganic CsPbI ₂ Br Perovskite Solar Cells. Solar Rrl, 2020, 4, 2000001.	3.1	29

#	Article	IF	CITATIONS
271	Microstructure and lattice strain control towards high-performance ambient green-printed perovskite solar cells. Journal of Materials Chemistry A, 2021, 9, 13297-13305.	5.2	29
272	Metalâ€Free Organic Halide Perovskite: A New Class for Next Optoelectronic Generation Devices. Advanced Energy Materials, 2021, 11, 2003331.	10.2	29
273	Holeâ€Storage Enhanced aâ€Si Photocathodes for Efficient Hydrogen Production. Angewandte Chemie - International Edition, 2021, 60, 11966-11972.	7.2	29
274	An in-situ defect passivation through a green anti-solvent approach for high-efficiency and stable perovskite solar cells. Science Bulletin, 2021, 66, 1419-1428.	4.3	29
275	2D-C ₃ N ₄ encapsulated perovskite nanocrystals for efficient photo-assisted thermocatalytic CO ₂ reduction. Chemical Science, 2022, 13, 1335-1341.	3.7	29
276	Beach-Chair-Shaped Energy Band Alignment for High-Performance β-CsPbI3 Solar Cells. Cell Reports Physical Science, 2020, 1, 100180.	2.8	28
277	Singleâ€Atom Doping and Highâ€Valence State for Synergistic Enhancement of NiO Electrocatalytic Water Oxidation. Small, 2021, 17, e2102448.	5.2	28
278	The effect of transparent conductive oxide on the performance CH3NH3PbI3 perovskite solar cell without electron/hole selective layers. Solar Energy, 2016, 135, 654-661.	2.9	27
279	Magnetic Field-Assisted Perovskite Film Preparation for Enhanced Performance of Solar Cells. ACS Applied Materials & Interfaces, 2017, 9, 21756-21762.	4.0	27
280	Interfacial TiO2 atomic layer deposition triggers simultaneous crystallization control and band alignment for efficient CsPbIBr2 perovskite solar cell. Organic Electronics, 2019, 74, 103-109.	1.4	27
281	Effect of TC(002) on the Output Current of a ZnO Thin-Film Nanogenerator and a New Piezoelectricity Mechanism at the Atomic Level. ACS Applied Materials & Interfaces, 2019, 11, 12656-12665.	4.0	27
282	Flexible Perowskit‣olarzellen: Herstellung und Anwendungen. Angewandte Chemie, 2019, 131, 4512-4530.	1.6	27
283	Double Side Interfacial Optimization for Lowâ€Temperature Stable CsPbI ₂ Br Perovskite Solar Cells with High Efficiency Beyond 16%. Energy and Environmental Materials, 2022, 5, 637-644.	7.3	27
284	Formamidinium-based Ruddlesden–Popper perovskite films fabricated <i>via</i> two-step sequential deposition: quantum well formation, physical properties and film-based solar cells. Energy and Environmental Science, 2022, 15, 1144-1155.	15.6	27
285	Polarity regulation for stable 2D-perovskite-encapsulated high-efficiency 3D-perovskite solar cells. Nano Energy, 2022, 95, 106965.	8.2	27
286	Protonâ€transferâ€induced in situ defect passivation for highly efficient wideâ€bandgap inverted perovskite solar cells. InformaÄnÃ-Materiály, 2022, 4, .	8.5	27
287	Stable Highâ€Efficiency CsPbI ₂ Br Solar Cells by Designed Passivation Using Multifunctional 2D Perovskite. Advanced Functional Materials, 2022, 32, .	7.8	27
288	Diameter regulated ZnO nanorod synthesis and its application in gas sensor optimization. Journal of Alloys and Compounds, 2014, 586, 436-440.	2.8	26

#	Article	IF	CITATIONS
289	Stoichiometry control of sputtered zinc oxide films by adjusting Ar/O2 gas ratios as electron transport layers for efficient planar perovskite solar cells. Solar Energy Materials and Solar Cells, 2018, 178, 200-207.	3.0	26
290	NaCl-assisted defect passivation in the bulk and surface of TiO2 enhancing efficiency and stability of planar perovskite solar cells. Journal of Power Sources, 2020, 448, 227586.	4.0	26
291	Surface Engineering to Reduce the Interfacial Resistance for Enhanced Photocatalytic Water Oxidation. ACS Catalysis, 2020, 10, 8742-8750.	5.5	26
292	Effective solvent-additive enhanced crystallization and coverage of absorber layers for high efficiency formamidinium perovskite solar cells. RSC Advances, 2016, 6, 56807-56811.	1.7	25
293	Design of surface termination for high-performance perovskite solar cells. Journal of Materials Chemistry A, 2021, 9, 23597-23606.	5.2	25
294	Carrier Generation Engineering toward 18% Efficiency Organic Solar Cells by Controlling Film Microstructure. Advanced Energy Materials, 2022, 12, .	10.2	25
295	Graphene oxide – a surprisingly good nucleation seed and adhesion promotion agent for one-step ZnO lithography and optoelectronic applications. Journal of Materials Chemistry C, 2014, 2, 8956-8961.	2.7	24
296	Au nanoparticle enhanced thin-film silicon solar cells. Solar Energy Materials and Solar Cells, 2016, 147, 225-234.	3.0	24
297	Shape―and Trapâ€Controlled Nanocrystals for Giantâ€Performance Improvement of Allâ€Inorganic Perovskite Photodetectors. Particle and Particle Systems Characterization, 2018, 35, 1700363.	1.2	24
298	In Situ Grain Boundary Modification via Two-Dimensional Nanoplates to Remarkably Improve Stability and Efficiency of Perovskite Solar Cells. ACS Applied Materials & Interfaces, 2018, 10, 39802-39808.	4.0	24
299	Highly efficient perovskite solar cells based on a dopant-free conjugated DPP polymer hole transport layer: influence of solvent vapor annealing. Sustainable Energy and Fuels, 2018, 2, 2154-2159.	2.5	24
300	Comprehensive investigation of sputtered and spin-coated zinc oxide electron transport layers for highly efficient and stable planar perovskite solar cells. Journal of Power Sources, 2019, 427, 223-230.	4.0	24
301	Double‣ite Ni–W Nanosheet for Best Alkaline HER Performance at High Current Density >500 mA cm ^{â^'2} . Advanced Materials Interfaces, 2019, 6, 1900308.	1.9	24
302	Deepâ€Level Transient Spectroscopy for Effective Passivator Selection in Perovskite Solar Cells to Attain High Efficiency over 23%. ChemSusChem, 2021, 14, 3182-3189.	3.6	24
303	Centimeter-Sized 2D Perovskitoid Single Crystals for Efficient X-ray Photoresponsivity. Chemistry of Materials, 2022, 34, 1699-1709.	3.2	24
304	Synergetic surface defect passivation towards efficient and stable inorganic perovskite solar cells. Chemical Engineering Journal, 2022, 447, 137515.	6.6	24
305	A Two‣tage Annealing Strategy for Crystallization Control of CH ₃ NH ₃ PbI ₃ Films toward Highly Reproducible Perovskite Solar Cells. Small, 2018, 14, e1800181.	5.2	23
306	Enhanced Visible-Light Photocatalytic H ₂ Evolution in Cu ₂ O/Cu ₂ Se Multilayer Heterostructure Nanowires Having {111} Facets and Physical Mechanism. Inorganic Chemistry, 2018, 57, 8019-8027.	1.9	23

#	Article	IF	CITATIONS
307	PbTiO ₃ as Electronâ€Selective Layer for Highâ€Efficiency Perovskite Solar Cells: Enhanced Electron Extraction via Tunable Ferroelectric Polarization. Advanced Functional Materials, 2019, 29, 1806427.	7.8	23
308	IrO _{<i>x</i>} @In ₂ O ₃ Heterojunction from Individually Crystallized Oxides for Weakâ€Lightâ€Promoted Electrocatalytic Water Oxidation. Angewandte Chemie - International Edition, 2021, 60, 26790-26797.	7.2	23
309	High detectivity photodetectors based on perovskite nanowires with suppressed surface defects. Photonics Research, 2020, 8, 1862.	3.4	23
310	One-pot synthesis of Co-doped ZnO hierarchical aggregate and its high gas sensor performance. Materials Chemistry and Physics, 2015, 149-150, 344-349.	2.0	22
311	Ag nanoparticle enhanced light trapping in hydrogenated amorphous silicon germanium solar cells on flexible stainless steel substrate. Solar Energy Materials and Solar Cells, 2016, 144, 63-67.	3.0	22
312	Perovskite as an effective V oc switcher for high efficiency polymer solar cells. Nano Energy, 2016, 20, 126-133.	8.2	22
313	Synthesis of a nano-sized hybrid C ₃ N ₄ /TiO ₂ sample for enhanced and steady solar energy absorption and utilization. Sustainable Energy and Fuels, 2017, 1, 95-102.	2.5	22
314	Improving sensing performance of the ZnO foam structure with exposed {001} facets by hydrogenation and sensing mechanism at molecule level. Applied Surface Science, 2019, 479, 646-654.	3.1	22
315	Superior Textured Film and Process Tolerance Enabled by Intermediateâ€State Engineering for Highâ€Efficiency Perovskite Solar Cells. Advanced Science, 2020, 7, 1903009.	5.6	22
316	Centimeterâ€Sized Molecular Perovskite Crystal for Efficient Xâ€Ray Detection. Advanced Functional Materials, 2021, 31, 2100691.	7.8	22
317	Secondary crystallization strategy for highly efficient inorganic CsPbI2Br perovskite solar cells with efficiency approaching 17%. Journal of Energy Chemistry, 2021, 63, 558-565.	7.1	22
318	Effect of Solvent Residue in the Thin-Film Fabrication on Perovskite Solar Cell Performance. ACS Applied Materials & Interfaces, 2022, 14, 28729-28737.	4.0	22
319	A straightforward chemical approach for excellent In ₂ S ₃ electron transport layer for high-efficiency perovskite solar cells. RSC Advances, 2019, 9, 884-890.	1.7	21
320	Roomâ€Temperature Surface Sulfurization for Highâ€Performance Kesterite CZTSe Solar Cells. Solar Rrl, 2019, 3, 1800236.	3.1	21
321	Perovskite/germanium tandem: A potential high efficiency thin film solar cell design. Optics Communications, 2016, 380, 1-5.	1.0	20
322	P-type sub-tungsten-oxide based urchin-like nanostructure for superior room temperature alcohol sensor. Applied Surface Science, 2018, 441, 277-284.	3.1	20
323	Moisture-Induced Crystallinity Improvement for Efficient CsPbl _{3–<i>x</i>} Br <i>_{<i>x</i>}</i> Perovskite Solar Cells with Excess Cesium Bromide. Journal of Physical Chemistry Letters, 2019, 10, 4587-4595.	2.1	20
324	Direct–Indirect Transition of Pressurized Two-Dimensional Halide Perovskite: Role of Benzene Ring Stack Ordering. Journal of Physical Chemistry Letters, 2019, 10, 5687-5693.	2.1	20

#	Article	IF	CITATIONS
325	Anorganische CsPbX ₃ â€Perowskitâ€&olarzellen: Fortschritte und Perspektiven. Angewandte Chemie, 2019, 131, 15742-15765.	1.6	20
326	Direct Growth of Pyramidâ€Textured Perovskite Single Crystals: A New Strategy for Enhanced Optoelectronic Performance. Advanced Functional Materials, 2020, 30, 2002742.	7.8	20
327	Superior photovoltaics/optoelectronics of two-dimensional halide perovskites. Journal of Energy Chemistry, 2021, 57, 69-82.	7.1	20
328	Self-assembled CoOOH on TiO2 for enhanced photoelectrochemical water oxidation. Journal of Energy Chemistry, 2021, 60, 512-521.	7.1	20
329	Highly Efficient and Stable CsPbTh ₃ (Th = I, Br, Cl) Perovskite Solar Cells by Combinational Passivation Strategy. Advanced Science, 2022, 9, e2105103.	5.6	20
330	All-Inorganic Perovskite Solar Cells with Tetrabutylammonium Acetate as the Buffer Layer between the SnO ₂ Electron Transport Film and CsPbI ₃ . ACS Applied Materials & Interfaces, 2022, 14, 5183-5193.	4.0	20
331	Enhanced sensing performance and sensing mechanism of hydrogenated NiO particles. Sensors and Actuators B: Chemical, 2017, 250, 208-214.	4.0	19
332	The sensing reaction on the Ni-NiO (111) surface at atomic and molecule level and migration of electron. Sensors and Actuators B: Chemical, 2018, 273, 794-803.	4.0	19
333	Nanoconfined Crystallization for Highâ€Efficiency Inorganic Perovskite Solar Cells. Small Science, 2021, 1, 2000054.	5.8	19
334	Post-treatment by an ionic tetrabutylammonium hexafluorophosphate for improved efficiency and stability of perovskite solar cells. Journal of Energy Chemistry, 2022, 64, 8-15.	7.1	19
335	Flexible perovskite solar cells: Material selection and structure design. Applied Physics Reviews, 2022, 9, .	5.5	19
336	Efficient Eco-Friendly Flexible X-ray Detectors Based on Molecular Perovskite. Nano Letters, 2022, 22, 5973-5981.	4.5	19
337	Photoassisted Hydrothermal Synthesis of IrOx–TiO ₂ for Enhanced Water Oxidation. ACS Sustainable Chemistry and Engineering, 2019, 7, 17941-17949.	3.2	18
338	Perovskite Solar Cells toward Eco-Friendly Printing. Research, 2021, 2021, 9671892.	2.8	18
339	Grain and stoichiometry engineering for ultra-sensitive perovskite X-ray detectors. Journal of Materials Chemistry A, 2021, 9, 25603-25610.	5.2	18
340	Inch-size Cs ₃ Bi ₂ I ₉ polycrystalline wafers with near-intrinsic properties for ultralow-detection-limit X-ray detection. Journal of Materials Chemistry C, 2022, 10, 6665-6672.	2.7	18
341	Waterâ€Resistant Leadâ€Free Perovskitoid Single Crystal for Efficient Xâ€Ray Detection. Advanced Functional Materials, 2022, 32, .	7.8	18
342	Enhancing the Performance of Amorphous‣ilicon Photoanodes for Photoelectrocatalytic Water Oxidation. ChemSusChem, 2015, 8, 3987-3991.	3.6	17

#	Article	IF	CITATIONS
343	Band alignment of TiO2/FTO interface determined by X-ray photoelectron spectroscopy: Effect of annealing. AIP Advances, 2016, 6, .	0.6	17
344	Local temperature reduction induced crystallization of MASnI ₃ and achieving a direct wafer production. RSC Advances, 2017, 7, 38155-38159.	1.7	17
345	Collaborative Strategy of Multifunctional Groups in Trifluoroacetamide Achieving Efficient and Stable Perovskite Solar Cells. Solar Rrl, 2022, 6, .	3.1	17
346	Size-dependent optical properties and enhanced visible light photocatalytic activity of wurtzite CdSe hexagonal nanoflakes with dominant {001} facets. Journal of Alloys and Compounds, 2014, 610, 62-68.	2.8	16
347	Green Atmospheric Aqueous Solution Deposition for High Performance Cu 2 ZnSn(S,Se) 4 Thin Film Solar Cells. Solar Rrl, 2018, 2, 1800233.	3.1	16
348	Verringerung schÃ e licher Defekte für leistungsstarke Metallhalogenidâ€Perowskitâ€Solarzellen. Angewandte Chemie, 2020, 132, 6740-6764.	1.6	16
349	Improved Interface Contact for Highly Stable All-Inorganic CsPbI ₂ Br Planar Perovskite Solar Cells. ACS Applied Energy Materials, 2020, 3, 5173-5181.	2.5	16
350	Anthradithiophene based hole-transport material for efficient and stable perovskite solar cells. Journal of Energy Chemistry, 2020, 48, 293-298.	7.1	16
351	Versatile Bidentate Chemical Passivation on a Cesium Lead Inorganic Perovskite for Efficient and Stable Photovoltaics. ACS Applied Energy Materials, 2021, 4, 4021-4028.	2.5	16
352	Diaminobenzene Dihydroiodideâ€MA _{0.6} FA _{0.4} PbI _{3â^'} <i>_x</i> Cl <i>_{xUnsymmetrical Perovskites with over 22% Efficiency for High Stability Solar Cells. Advanced Functional Materials, 2022, 32, .}</i>	b≥7.8	16
353	p-Layer bandgap engineering for high efficiency thin film silicon solar cells. Materials Science in Semiconductor Processing, 2015, 39, 192-199.	1.9	15
354	Highly thermally stable and emission color tunable borate glass for whiteâ€lightâ€emitting diodes with zero organic resin. Journal of the American Ceramic Society, 2017, 100, 4011-4020.	1.9	15
355	Chelate-Pb Intermediate Engineering for High-Efficiency Perovskite Solar Cells. ACS Applied Materials & Interfaces, 2018, 10, 14744-14750.	4.0	15
356	Electronic and magnetic behaviors of B, N, and 3d transition metal substitutions in germanium carbide monolayer. Journal of Magnetism and Magnetic Materials, 2018, 451, 799-807.	1.0	15
357	Morphology Evolution of a Highâ€Efficiency PSC by Modulating the Vapor Process. Small, 2020, 16, e2003582.	5.2	15
358	High‣fficiency Perovskite Solar Cells Enabled by Anatase TiO ₂ Nanopyramid Arrays with an Oriented Electric Field. Angewandte Chemie, 2020, 132, 12067-12074.	1.6	15
359	Sequential Formation of Tunableâ€Bandgap Mixedâ€Halide Leadâ€Based Perovskites: In Situ Investigation and Photovoltaic Devices. Solar Rrl, 2021, 5, .	3.1	15
360	Semitransparent Flexible Perovskite Solar Cells for Potential Greenhouse Applications. Solar Rrl, 2021, 5, 2100264.	3.1	15

#	Article	IF	CITATIONS
361	Lead-free molecular one-dimensional perovskite for efficient X-ray detection. Journal of Energy Chemistry, 2022, 64, 209-213.	7.1	15
362	lonâ€Accumulationâ€Induced Charge Tunneling for High Gain Factor in P–l–Nâ€Structured Perovskite CH ₃ NH ₃ PbI ₃ Xâ€Ray Detector. Advanced Materials Technologies, 2022, 7, 2100908.	3.0	15
363	Rational Design of Heterojunction Interface for Cu ₂ ZnSn(S,Se) ₄ Solar Cells to Exceed 12% Efficiency. Solar Rrl, 2022, 6, .	3.1	15
364	Synergistic Effect of Anti‣olvent and Component Engineering for Effective Passivation to Attain Highly Stable Perovskite Solar Cells. Solar Rrl, 2022, 6, .	3.1	15
365	Millimeter-long multilayer graphene nanoribbons prepared by wet chemical processing. Carbon, 2014, 71, 120-126.	5.4	14
366	Hydrogenated TiO2 nanosheet based flowerlike architectures: Enhanced sensing performances and sensing mechanism. Journal of Alloys and Compounds, 2018, 749, 543-555.	2.8	14
367	Improving the Quality of CH ₃ NH ₃ PbI ₃ Films via Chlorobenzene Vapor Annealing. Physica Status Solidi (A) Applications and Materials Science, 2018, 215, 1700959.	0.8	14
368	Giant Phonon Tuning Effect via Pressure-Manipulated Polar Rotation in Perovskite MAPbI ₃ . Journal of Physical Chemistry Letters, 2018, 9, 3029-3034.	2.1	14
369	Black Phosphorusâ€Based Compound with Few Layers for Photocatalytic Water Oxidation. ChemCatChem, 2018, 10, 3424-3428.	1.8	14
370	Highâ€Efficiency Perovskite Solar Cells with Imidazoliumâ€Based Ionic Liquid for Surface Passivation and Charge Transport. Angewandte Chemie, 2021, 133, 4284-4290.	1.6	14
371	Interfaces and Interfacial Layers in Inorganic Perovskite Solar Cells. Angewandte Chemie, 2021, 133, 26644-26657.	1.6	14
372	Inner Strain Regulation in Perovskite Single Crystals through Fine-Tuned Halide Composition. Crystal Growth and Design, 2021, 21, 1741-1750.	1.4	14
373	InOCl nanosheets with exposed {001} facets: Synthesis, electronic structure and surprisingly high photocatalytic activity. Applied Catalysis B: Environmental, 2014, 152-153, 390-396.	10.8	13
374	Fabrication gallium/graphene core–shell nanoparticles by pulsed laser deposition and their applications in surface enhanced Raman scattering. Materials Letters, 2015, 143, 194-196.	1.3	13
375	Photoinduced surface voltage mapping study for large perovskite single crystals. Applied Physics Letters, 2016, 108, 181604.	1.5	13
376	Multiple-Stage Structure Transformation of Organic-Inorganic Hybrid Perovskite <mml:math xmlns:mml="http://www.w3.org/1998/Math/MathML" display="inline"><mml:mrow><mml:msub><mml:mrow><mml:mi>CH</mml:mi></mml:mrow><mml:mrow><mr Physical Review X, 2016, 6, .</mr </mml:mrow></mml:msub></mml:mrow></mml:math 	nl:mn8>3 </td <td>18 mml:mn> </td>	18 mml:mn>
377	Simultaneous dual-interface and bulk defect passivation for high-efficiency and stable CsPbI2Br perovskite solar cells. Journal of Power Sources, 2021, 492, 229580.	4.0	13
378	Superior texture-controlled ZnO thin film using electrochemical deposition. Solar Energy, 2016, 125, 192-197.	2.9	12

#	Article	IF	CITATIONS
379	Origin of enhanced stability in thiocyanate substituted α-FAPbI3 analogues. Science China Chemistry, 2019, 62, 866-874.	4.2	12
380	Interface Modification of a Perovskite/Hole Transport Layer with Tetraphenyldibenzoperiflanthene for Highly Efficient and Stable Solar Cells. ACS Applied Materials & Interfaces, 2020, 12, 45073-45082.	4.0	12
381	High-efficiency and thermal/moisture stable CsPbI _{2.84} Br _{0.16} inorganic perovskite solar cells enabled by a multifunctional cesium trimethylacetate organic additive. Journal of Materials Chemistry A, 2021, 9, 4922-4932.	5.2	12
382	Dualâ€Interface Modification of CsPblBr ₂ Solar Cells with Improved Efficiency and Stability. Advanced Materials Interfaces, 2021, 8, 2001994.	1.9	12
383	Alkyl Diamine-Induced (100)-Preferred Crystal Orientation for Efficient Pb–Sn Perovskite Solar Cells. ACS Applied Energy Materials, 2022, 5, 6936-6942.	2.5	12
384	Facile synthesis of "lucky clover―hole-transport material for efficient and stable large-area perovskite solar cells. Journal of Power Sources, 2020, 454, 227938.	4.0	11
385	Enabling Unassisted Solar Water Splitting by Single-Junction Amorphous Silicon Photoelectrodes. ACS Applied Energy Materials, 2020, 3, 4629-4637.	2.5	11
386	Highly stable and efficient perovskite solar cells produced via high-boiling point solvents and additive engineering synergistically. Science China Chemistry, 2020, 63, 818-826.	4.2	11
387	van der Waals Interaction-Induced Tunable Schottky Barriers in Metal–2D Perovskite Contacts. Journal of Physical Chemistry Letters, 2021, 12, 1718-1725.	2.1	11
388	Centimeterâ€Sized Single Crystal of Twoâ€Dimensional Halide Perovskites Incorporating Straightâ€Chain Symmetric Diammonium Ion for Xâ€Ray Detection. Angewandte Chemie, 2020, 132, 15006-15012.	1.6	11
389	Optical and electrical properties of high-quality Ti2O3 epitaxial film grown on sapphire substrate. Applied Physics A: Materials Science and Processing, 2016, 122, 1.	1.1	10
390	Highly stabilized perovskite solar cell prepared using vacuum deposition. RSC Advances, 2016, 6, 93525-93531.	1.7	10
391	Investigation of the mechanism responsible for the photoluminescence enhancement with Li + co-doping in highly thermally stable white-emitting Sr 8 ZnSc(PO 4) 7 :Dy 3+ phosphor. Journal of Luminescence, 2017, 187, 160-168.	1.5	10
392	Monolayer-by-monolayer growth of platinum films on complex carbon fiber paper structure. Applied Surface Science, 2017, 407, 386-390.	3.1	10
393	The photovoltaic effect in a [001] orientated ZnO thin film and its physical mechanism. RSC Advances, 2017, 7, 9596-9604.	1.7	10
394	Ge quantum-dot enhanced c-Si solar cell for improved light trapping efficiency. Solar Energy, 2018, 167, 102-107.	2.9	10
395	Pseudohalide induced tunable electronic and excitonic properties in two-dimensional single-layer perovskite for photovoltaics and photoelectronic applications. Journal of Energy Chemistry, 2019, 36, 106-113.	7.1	10
396	Improvement of Colloidal Characteristics in a Precursor Solution by a PbI2-(DMSO)2 Complex for Efficient Nonstoichiometrically Prepared CsPbI2.8Br0.2 Perovskite Solar Cells. ACS Applied Materials & Interfaces, 2020, 12, 48756-48764.	4.0	10

#	Article	IF	CITATIONS
397	The Possible Side Reaction in the Annealing Process of Perovskite Layers. ACS Applied Materials & Interfaces, 2020, 12, 35043-35048.	4.0	10
398	Cd-Doped Triple-Cation Perovskite Thin Films with a 20 μs Carrier Lifetime. Journal of Physical Chemistry C, 2020, 124, 22011-22018.	1.5	10
399	Triphenylamine-based hole transporting materials with thiophene-derived bridges for perovskite solar cells. Synthetic Metals, 2020, 261, 116323.	2.1	10
400	4â€Hydrazinobenzoicâ€Acid Antioxidant for Highâ€Efficiency Sn–Pb Alloyed Perovskite Solar Cells. Energy Technology, 2022, 10, .	1.8	10
401	Balanced-Strength Additive for High-Efficiency Stable Perovskite Solar Cells. ACS Applied Energy Materials, 2022, 5, 8034-8041.	2.5	10
402	Controlled Pt Monolayer Fabrication on Complex Carbon Fiber Structures for Superior Catalytic Applications. Electrochimica Acta, 2016, 222, 1522-1527.	2.6	9
403	Flowerlike Cu ₂ Te architectures constructed from ultrathin nanoflakes as superior dye adsorbents for wastewater treatment. RSC Advances, 2016, 6, 79612-79619.	1.7	9
404	Superior Cu 2 S/brass-mesh electrode in CdS quantum dot sensitized solar cells for dual-side illumination. Materials Letters, 2017, 195, 100-103.	1.3	9
405	Single-crystalline perovskite wafers with a Cr blocking layer for broad and stable light detection in a harsh environment. RSC Advances, 2018, 8, 14848-14853.	1.7	9
406	Fabrication of a High-Quality Cu ₂ ZnSn(S,Se) ₄ Absorber Layer via an Aqueous Solution Process and Application in Solar Cells. ACS Applied Materials & Interfaces, 2019, 11, 634-639.	4.0	9
407	Hot Debate on Perovskite Solar Cells: Stability, Toxicity, High-Efficiency and Low Cost. Journal of Energy Chemistry, 2021, 53, 407-411.	7.1	9
408	The effects of Ag particle morphology on the antireflective properties of silicon textured using Ag-assisted chemical etching. Journal of Alloys and Compounds, 2016, 670, 156-160.	2.8	8
409	Abnormal absorption onset shift of CH3NH3PbI3 film by adding PbBr2 into its precursor and its effect on photovoltaic performance. Journal of Power Sources, 2019, 437, 226914.	4.0	8
410	Oxidation, reduction, and inert gases plasma-modified defects in TiO2 as electron transport layer for planar perovskite solar cells. Journal of CO2 Utilization, 2019, 32, 46-52.	3.3	8
411	Influence of Film Quality on Power Conversion Efficiency in Perovskite Solar Cells. Coatings, 2019, 9, 622.	1.2	8
412	Breaking Platinum Nanoparticles to Singleâ€Atomic Ptâ€C 4 Coâ€catalysts for Enhanced Solarâ€toâ€Hydrogen Conversion. Angewandte Chemie, 2021, 133, 2571-2577.	1.6	8
413	Pyrenesulfonic Acid Sodium Salt for Effective Bottom‣urface Passivation to Attain High Performance of Perovskite Solar Cells. Solar Rrl, 2021, 5, 2100416.	3.1	8
414	Structural and Functional Insights into Metal-Free Perovskites. Journal of Physical Chemistry Letters, 2022, 13, 5168-5178.	2.1	8

#	Article	IF	CITATIONS
415	Solarâ€ŧoâ€Hydrogen Efficiency of 9.5 % by using a Thin‣ayer Platinum Catalyst and Commercial Amorphous Silicon Solar Cells. ChemCatChem, 2016, 8, 1713-1717.	1.8	7
416	Cellular Architectureâ€Based Allâ€Polymer Flexible Thinâ€Film Photodetectors with High Performance and Stability in Harsh Environment. Advanced Materials Technologies, 2017, 2, 1700185.	3.0	7
417	A temperature gradient-induced directional growth of a perovskite film. Journal of Materials Chemistry A, 2020, 8, 17019-17024.	5.2	7
418	Ultrastable Perovskite–Zeolite Composite Enabled by Encapsulation and Inâ€Situ Passivation. Angewandte Chemie, 2020, 132, 23300-23306.	1.6	7
419	Photogenerated Charge Separation between Polar Crystal Facets Under a Spontaneous Electric Field. Advanced Optical Materials, 2021, 9, 2001898.	3.6	7
420	Enabling Solar Hydrogen Production over Selenium: Surface State Passivation and Cocatalyst Decoration. ACS Sustainable Chemistry and Engineering, 2021, 9, 9923-9931.	3.2	7
421	Thickness Influence on Optical and Electrical Properties of PbI2 Films Prepared by Pulsed Laser Deposition. Science of Advanced Materials, 2018, 10, 701-706.	0.1	7
422	Effective surface passivation with 4-bromo-benzonitrile to enhance the performance of perovskite solar cells. Journal of Materials Chemistry C, 2021, 9, 17089-17098.	2.7	7
423	In-situ photoisomerization of azobenzene to inhibit ion-migration for stable high-efficiency perovskite solar cells. Journal of Energy Chemistry, 2022, 73, 556-564.	7.1	7
424	Generation and manipulation of higher order Fano resonances in plasmonic nanodisks with a built-in missing sectorial slice. Europhysics Letters, 2013, 104, 47009.	0.7	6
425	Ge quantum dot enhanced hydrogenated amorphous silicon germanium solar cells on flexible stainless steel substrate. Solar Energy, 2017, 144, 635-642.	2.9	6
426	Exposed the mechanism of lead chloride dopant for high efficiency planar-structure perovskite solar cells. Organic Electronics, 2018, 62, 499-504.	1.4	6
427	Synergistic enhancement of Cs and Br doping in formamidinium lead halide perovskites for high performance optoelectronics. CrystEngComm, 2018, 20, 5510-5518.	1.3	6
428	Effective electron extraction from active layer for enhanced photodetection of photoconductive type detector with structure of Au/CH3NH3PbI3/Au. Organic Electronics, 2019, 74, 197-203.	1.4	6
429	Increasing gas sensitivity of Co3O4 octahedra by tuning Co-Co3O4 (111) surface structure and sensing mechanism of 3-coordinated Co atom as an active center. Journal of Materials Science: Materials in Electronics, 2020, 31, 8852-8864.	1.1	6
430	Room-temperature sputtered-SnO2 modified anode toward efficient TiO2-based planar perovskite solar cells. Science China Technological Sciences, 2021, 64, 1995-2002.	2.0	6
431	Fabrication of a Cu2MnSn(S,Se)4thin film based on a low-cost degradable solution process. CrystEngComm, 2016, 18, 4744-4748.	1.3	5
432	Modeling of triangular-shaped substrates for light trapping in microcrystalline silicon solar cells. Optics Communications, 2017, 383, 304-309.	1.0	5

#	Article	IF	CITATIONS
433	"Heat Wave―of Metal Halide Perovskite Solar Cells Continues in Phoenix. ACS Energy Letters, 2018, 3, 1898-1903.	8.8	5
434	Perspective on the imaging device based on perovskite materials. Journal of Semiconductors, 2020, 41, 050401.	2.0	5
435	ASnX ₃ —Better than Pbâ€based Perovskite. Nano Select, 2021, 2, 159-186.	1.9	5
436	Improving Performance and Stability of Planar Perovskite Solar Cells Through Passivation Effect with Green Additives. Solar Rrl, 2021, 5, 2000732.	3.1	5
437	Tapered Coaxial Arrays for Photon―and Plasmonâ€Enhanced Light Harvesting in Perovskite Solar Cells: A Theoretical Investigation Using the Finite Element Method. ChemPlusChem, 2021, 86, 858-864.	1.3	5
438	Imidazolium-based ionic liquid for stable and highly efficient black-phase formamidinium-based perovskite solar cell. Chemical Engineering Journal, 2022, 434, 134759.	6.6	5
439	Effect of Ag Film Thickness on the Morphology and Light Scattering Properties of Ag Nanoparticles. Nanoscience and Nanotechnology Letters, 2014, 6, 392-397.	0.4	4
440	Synthesis of hierarchical structure Cu2SnSe3 microsphere by a solvothermal method. Materials Letters, 2015, 161, 727-730.	1.3	4
441	Improvement of crystallinity for poly-Si thin film by negative substrate bias at low temperature. Thin Solid Films, 2017, 629, 90-96.	0.8	4
442	Lowâ€Temperatureâ€Processed CdS as the Electron Selective Layer in an Organometal Halide Perovskite Photovoltaic Device. Particle and Particle Systems Characterization, 2018, 35, 1800137.	1.2	4
443	IrO _{<i>x</i>} @In ₂ O ₃ Heterojunction from Individually Crystallized Oxides for Weak‣ightâ€Promoted Electrocatalytic Water Oxidation. Angewandte Chemie, 2021, 133, 26994-27001.	1.6	4
444	Hydrazide Derivatives for Defect Passivation in Pure CsPbI3 Perovskite Solar Cells. Angewandte Chemie, 0, , .	1.6	4
445	First observation of magnon transport in organic-inorganic hybrid perovskite. Matter, 2022, , .	5.0	4
446	12.0% Efficiency on large area, encapsulated, multijunction nc-Si:H based solar cells. , 2011, , .		3
447	The Photoluminescence Behaviors of a Novel Reddish Orange Emitting Phosphor Caln ₂ O ₄ :Sm ³⁺ Codoped with Zn ²⁺ or Al ³⁺ Ions. Journal of Nanomaterials, 2015, 2015, 1-5.	1.5	3
448	Controlled electrodeposition of Au monolayer film on ionic liquid. Applied Surface Science, 2016, 371, 258-261.	3.1	3
449	H2-Ar dilution for improved c-Si quantum dots in P-doped SiNx:H thin film matrix. Applied Surface Science, 2017, 396, 235-242.	3.1	3
450	Unraveling the crucial role of spacer ligands in tuning the contact properties of metal–2D perovskite interfaces. Journal of Materials Chemistry C, 2021, 9, 8489-8495.	2.7	3

#	Article	IF	CITATIONS
451	Synergistic Effect of RbBr Interface Modification on Highly Efficient and Stable Perovskite Solar Cells. ACS Omega, 2021, 6, 13766-13773.	1.6	3
452	Cation Engineering for Effective Defect Passivation to Improve Efficiency and Stability of FA0.5MA0.5PbI3 Perovskite Solar Cells. ACS Applied Energy Materials, 2021, 4, 7654-7660.	2.5	3
453	Utilizing the Energy Transfer of Ce ⁴⁺ – and Ce ³⁺ –Tb ³⁺ to Boost the Luminescence Quantum Efficiency up to 100% in Borate Glass. Journal of Physical Chemistry C, 2022, 126, 5838-5846.	1.5	3
454	Amino Acidâ€Based Lowâ€Dimensional Management for Enhanced Perovskite Solar Cells. Solar Rrl, 2022, 6,	3.1	3
455	Lateral matching of periodic front and back textures in thin film silicon solar cells. Optics Communications, 2015, 357, 28-33.	1.0	2
456	Ag Nanoparticle Enhanced Flexible Thin-Film Silicon Solar Cells. Journal of Nanoscience and Nanotechnology, 2017, 17, 3689-3694.	0.9	2
457	Sputtered ZnO Films as Electron Transport Layers for Efficient Planar Perovskite Solar Cells. , 2018, , .		2
458	Synergistically Enhanced Amplified Spontaneous Emission by Cd Doping and Clâ€Assisted Crystallization. Advanced Optical Materials, 2021, 9, 2001825.	3.6	2
459	Holeâ€Storage Enhanced aâ€Si Photocathodes for Efficient Hydrogen Production. Angewandte Chemie, 2021, 133, 12073-12079.	1.6	2
460	Fabrication and Light Scattering Properties of Size Controlled Aluminum Surface Periodic Nanopits. Nanoscience and Nanotechnology Letters, 2014, 6, 470-476.	0.4	2
461	Flexible Diodes/Transistors Based on Tunable p-n-Type Semiconductivity in Graphene/Mn-Co-Ni-O Nanocomposites. Research, 2021, 2021, 9802795.	2.8	2
462	Roles of Organic Ligands in Ambient Stability of Layered Halide Perovskites. ACS Applied Materials & Interfaces, 2022, 14, 33085-33093.	4.0	2
463	AFORS-HET simulation study of HIT solar cells: Significance of inversion layer. , 2016, , .		1
464	Effect of argon flow on promoting boron doping for <i>in-situ</i> grown silicon nitride thin films containing silicon quantum dots. Nanotechnology, 2017, 28, 285202.	1.3	1
465	Magnetic Field Driven Larger Grain Growth for Perovskite Film with Enhanced Photovoltaic Performance. , 2018, , .		1
466	Nanodevices: Record-Low-Threshold Lasers Based on Atomically Smooth Triangular Nanoplatelet Perovskite (Adv. Funct. Mater. 2/2019). Advanced Functional Materials, 2019, 29, 1970012.	7.8	1
467	Enhanced visible-light photocatalytic activity of hydrogenated Fe3O4 nanooctahedrons with {111} polar facets in degradation of Basic Fuchsin and the photocatalytic mechanism. Journal of Materials Science: Materials in Electronics, 2022, 33, 13095-13109.	1.1	1
468	Effective strategy for stabilized perovskite solar cells using tandem architecture. , 2015, , .		0

27

#	Article	IF	CITATIONS
469	Controllable synthesis of silicon nano-particles using a one-step PECVD-ionic liquid strategy. Journal of Materials Chemistry A, 2015, 3, 10233-10237.	5.2	0
470	Intrinsic Raman signatures of pristine hybrid perovskite CH ₃ NH ₃ PbI ₃ and its multiple stages of structure transformation. , 2016, , .		0
471	Stable high efficiency perovskite solar cells using vacuum deposition. , 2016, , .		Ο
472	Effect of nanopits size and spacing on the light absorption in silicon thin film solar cells. Optik, 2016, 127, 1003-1006.	1.4	0
473	Reply to â€~Comment on "Zero-thermal-quenching and photoluminescence tuning with the assistance of carriers from defect cluster trapsâ€â€™. Journal of Materials Chemistry C, 2020, 8, 1153-1156.	2.7	0
474	Optical Properties of Multilayered Ge Nanocrystals Embedded in SiO <i>_x</i> GeN <i>_y</i> Thin Films. Journal of Nanoscience and Nanotechnology, 2017, 17, 3519-3522.	0.9	0
475	Graphene–MCN pn-junction for ultrafast flexible ultraviolet detector. MRS Communications, 2021, 11, 862.	0.8	Ο